JOURNAL OF SOLID STATE CHEMISTRY 71, 87–94 (1987)

# Intrachain Exchange Energies in 1-Dimensional Magnetic Fluoromanganates(III) as a Function of Mn–F–Mn Bridge Angle and Crystal Structure of $Li_2MnF_5$

J. PEBLER, W. MASSA, H. LASS, AND B. ZIEGLER

*Fachbereich Chemie und Sonderforschungsbereich 127 (Kristallstruktur und Chemische Bindung) der Universität Marburg, Hans-Meerwein-Strasse, D-3550 Marburg, West Germany*

Received September 22, 1986; in revised form January 14, 1987

Seven pentafluoromanganates(III) $A^I_2MnF_5$ ($A$ = Li, Na, $NH_4$), $A^I_2MnF_5 \cdot H_2O$ ($A$ = Rb, Cs), and $A^{II}MnF_5 \cdot H_2O$ ($A$ = Sr, Ba) with linear chain structures of trans-connected $[MnF_6]$ octahedra have been used as model compounds for investigating the correlation of one-dimensional antiferromagnetic exchange energy and bridge angle. The crystal structure of $Li_2MnF_5$ was determined by X-ray diffraction (space group $C2/c$, $Z = 4$, $a = 10.016(1)$, $b = 4.948(1)$, $c = 7.408(1)$ Å, $\beta = 112.19(1)°$, $R_w = 0.019$ for 605 reflections). The bridge angle Mn–F–Mn is dependent upon the cation and varies between 121.5° in this Li compound and 180° in $Cs_2MnF_5 \cdot H_2O$. The magnetic properties have been analyzed by use of both high- and low-temperature theoretical methods. Above 10 K, the susceptibility is essentially that of a system with weak antiferromagnetic coupling by nearest-neighbor Heisenberg exchange interaction within an extended linear chain. The absolute value of the intrachain exchange energy $J/k$ depends to a marked extent upon the Mn–F–Mn bridge angle $\beta$ rather than on the Mn–Mn or Mn–F distances. With decreasing angle $\beta$, the antiferromagnetic interactions obviously decrease as $\cos^2(\beta)$ owing to a decrease in the $\sigma$-overlap of the $d_{z^2}$ and $p_z$ orbitals involved in a superexchange mechanism. 

## Introduction

The magnetic properties of a system of paramagnetic ions coupled in infinite linear chains by nearest-neighbor exchange interaction have been studied theoretically in several approximations (*1–4*). This treatment to calculate the magnetic properties of one-dimensional systems is mathematically simpler and more rigorous than that for two- or three-dimensional lattices. Accordingly, a large amount of experimental and theoretical work has been performed on various types of linear magnetism, resulting in valuable results for understanding magnetic interaction (for review see (*5*)).

Due to their relatively simple structural and bonding properties, transition metal fluorides play an important role as model compounds for magnetic studies (*5, 6*). In this work we use the family of pentafluoromanganates(III) $A^I_2MnF_5(\cdot H_2O)$ and $A^{II}MnF_5 \cdot H_2O$ with linear "trans-chain" structures for studies of the dependence on bridge angle Mn–F–Mn of the intrachain exchange energy. The structural properties



0022-4596/87 $3.00

TABLE I

ATOMIC FRACTIONAL COORDINATES AND TEMPERATURE FACTORS[a] FOR $Li_2MnF_5$

| Atom | $x$ | $y$ | $z$ | $U_{11}$ | $U_{22}$ | $U_{33}$ | $U_{23}$ | $U_{13}$ | $U_{12}$ |
|---|---|---|---|---|---|---|---|---|---|
| Mn | 0 | 0 | 0 | 0.0088(1) | 0.0073(1) | 0.0077(1) | 0.0001(1) | 0.0027(1) | −0.0002(1) |
| Li | 0.1385(3) | 0.5092(8) | 0.2493(5) | 0.0173(10) | 0.0173(11) | 0.0318(14) | 0.0038(17) | 0.0115(10) | 0.0010(14) |
| F1 | 0.0866(1) | 0.3075(2) | −0.0442(1) | 0.0184(4) | 0.0117(4) | 0.0177(4) | 0.0006(3) | 0.0099(3) | −0.0034(3) |
| F2 | 0.1772(1) | −0.1516(2) | 0.1456(1) | 0.0103(3) | 0.0141(4) | 0.0147(4) | 0.0023(3) | 0.0018(3) | 0.0016(3) |
| F3 | 0 | 0.2098(3) | 1/4 | 0.0164(5) | 0.0105(5) | 0.0094(5) | 0 | 0.0062(4) | 0 |

[a] Defined by $T = \exp\{2\pi^2(U_{11}h^2a^{*2} + \ldots + 2U_{23}klb^*c^*)\}$ (Å$^2$).

have been elucidated during the last few years (Table III). They all show linear chain anions built up by Jahn–Teller distorted $MnF_6^{3-}$ octahedra sharing trans vertices. While the geometry of the octahedra remains approximately constant, the bridge angle $\beta$ varies with the size of $A$ cations from 180° down to 121.5°. The latter smallest angle has now been found in $Li_2MnF_5$, whose crystal structure is dealt with in the first part of this work.

In the second part we present the results of measurements of the magnetic susceptibility performed on polycrystalline fluoromanganates(III). From these results we derive the intrachain exchange interaction among the manganese(III) ions. As we shall see, these results indicate that the intrachain exchange interaction depends to a marked extent on the Mn–F–Mn angle rather than the Mn–Mn or Mn–F distance.

## Crystal Structures

### *Structure Determination of $Li_2MnF_5$*

$Li_2MnF_5$ has been prepared by solid-state reaction of a stoichiometric mixture of LiF and $MnF_3$ in a sealed Pt tube (16 hr at 700°C, 1 hr at 800°C, cooling down by 50°/hr). A red single crystal of 0.13 × 0.07 × 0.05 mm$^3$ was used for X-ray film exposures and intensity measurements on a 4-circle diffractometer (CAD4, Enraf–Nonius, graphite monochromated Mo$K_\alpha$ radiation). The space group is $C2/c$ with $Z = 4$ and the lattice parameters were refined with 25 high-angle reflections to $a = 10.016(1)$, $b = 4.948(1)$, $c = 7.408(1)$ Å, $\beta = 112.19(1)°$; $d_c = 3.200$ g cm$^{-3}$. We have recorded 789 reflections in the range $\theta = 2$–$35°$ ($\pm h$, $k$, $l$, 741 independent, measuring time variable, max. 40 sec/reflection) using $\omega$-scans over $(0.9 + 0.35 \text{ tg } \theta)°$ and, in addition, 25% before and after the reflection for background determination. For these calculations, 605 reflections with $F_o > 3\sigma$ have been used. in the final stages of analysis, reflection 402 was suppressed because of probable Renninger effect. Due to the small crystal size at $\mu = 36.9$ cm$^{-1}$, no absorption correction has been applied.

The structure was solved by the Patterson method and refined with anisotropic temperature factors to $R_w = \Sigma \sqrt{w}\, \Delta / \Sigma \sqrt{w}\, |F_o| = 0.019$, $R_g = (\Sigma w \Delta^2 / \Sigma w F_o^2)^{1/2} = 0.021$ ($\Delta = \| |F_o| - |F_c| \|$, $w = 1.9/\sigma^2(F_o)$) using scattering factors for ions (*7*). An anomalous dispersion correction (*8*) was included and an empirical extinction parameter $\varepsilon = 3.0 \times 10^{-6}$ was refined. All calculations have been carried out in the system STRUX (*9*) on a Sperry 1100/62 computer at the HRZ Marburg with programs SHELX76 (*10*) and ORTEP (*11*). The resulting atomic parameters are tabulated in Table I, with bond lengths and angles in Table II.[1]

[1] Listings of the structure factors are obtainable from Fachinformationszentrum Energie Physik Mathematik GmbH, D-7514 Eggenstein-Leopoldshafen 2, West Germany, under specification of deposit No. CSDTCSD-52411, authors, and journal reference.

TABLE II

INTERATOMIC DISTANCES (Å) AND ANGLES (°) IN $Li_2MnF_5$

| | | | |
|---|---|---|---|
| Mn–F1 | 1.841(1) | F1–Mn–F2 | 91.5(1) |
| Mn–F2 | 1.852(1) | F1–Mn–F3 | 84.6(1) |
| Mn–F3 | 2.123(1) | F2–Mn–F3 | 90.3(1) |
| | | Mn–F3–Mn′ | 121.5(1) |
| Li–F1 | 2.267(4) | | |
| Li–F1′ | 2.372(4) | | |
| Li–F1″ | 2.008(4) | Mean value | |
| Li–F2 | 1.945(4) | | |
| Li–F2′ | 1.887(4) | Mn–F | 1.939 |
| Li–F3 | 2.031(4) | Li–F | 2.085 |

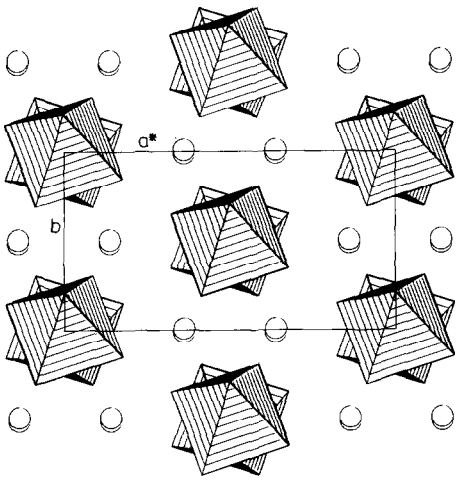


FIG. 1. Structure of $Li_2MnF_5$ projected from the chain direction [0010]. [$MnF_6$] groups are shown as solid octahedra and Li ions as circles.

### *Discussion of the Structure of $Li_2MnF_5$*

The structure of $Li_2MnF_5$ consists of parallel infinite chains of trans-corner-connected [$MnF_6$] octahedra oriented along the *c*-axis (Fig. 2). The chain packing derives from the hexagonal rod packing. Due to the strong Jahn–Teller effect of the $d^4$ high-spin configuration of Mn(III), the octahedra are remarkably lengthened in the bridging direction (Figs. 1 and 2). The bond lengths are approximately the same as in the other "trans-chain" fluoromanganates(III) (Table III), but the bridge angle Mn–F–Mn ($\beta$ = 121.5°) is the smallest among this class of compounds. This must be attributed to the tendency of $Li^+$ to adopt the coordination number 6 by bending of the chains. The strongly distorted [$LiF_6$] octahedra share common faces to form double units with a Li–Li distance of 2.778 Å, and are further connected via corners.

### *Experimental and Structural Data of the Fluoromanganates(III) Taken for Magnetic Investigations*

Replacing Li by the higher alkali or by alkaline earth ions yields similar trans chain compounds, in part hydrated, with increas-

TABLE III

STRUCTURAL DATA OF trans-CHAIN FLUOROMANGANATES (III)

| Compound | Space group | Structural type[a] | Mn–$F_{bridge}$ (Å) | Mn–$F_{term}$ (Å) | Mn–Mn (Å) | $\beta$ bridge angle (°) | Ref. |
|---|---|---|---|---|---|---|---|
| $Li_2MnF_5$ | *C2/c* | H | 2.123 | 1.847 | 3.70 | 121.5 | This work |
| $Na_2MnF_5$ | $P2_1/c$ | H | 2.109 | 1.849 | 3.86 | 132.5 | *14* |
| $SrMnF_5 \cdot H_2O$ | $P2_1/m$ | H | 2.108 | 1.845 | 3.96 | 139.8 | *16* |
| $(NH_4)_2MnF_5$ | *Pnma* | H | 2.091 | 1.853 | 3.97 | 143.4 | *15* |
| $BaMnF_5 \cdot H_2O$ | $P2_1/m$ | H | 2.127 | 1.854 | 4.09 | 147.7 | *16* |
| $Rb_2MnF_5 \cdot H_2O$ | *Cmcm* | T | 2.089 | 1.848 | 4.17 | 175.4 | *17* |
| $Cs_2MnF_5 \cdot H_2O$ | *Cmmm* | T | 2.130 | 1.836 | 4.26 | 180.0 | *13, 12* |
| $KMnF_4 \cdot H_2O$ | *C2/c* | H | 2.131<br>1.916 | 1.794<br>2.153 | 3.87 | 137.7 | *30* |

[a] H = Deriving from pseudohexagonal, T = from tetragonal chain packing.

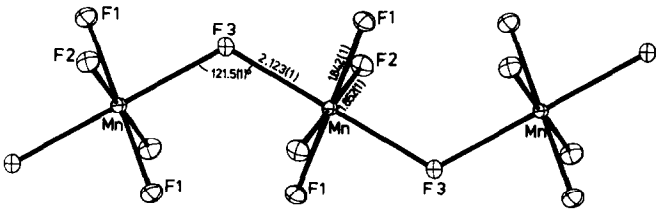


FIG. 2. Geometry of the infinite kinked "trans-chain" anions in $Li_2MnF_5$. Distances are in Å. Thermal ellipsoids at the 50% probability level.

ing bridge angle $\beta$ up to 180° for $Cs_2MnF_5$ (*12*) and $Cs_2MnF_5 \cdot H_2O$ (*13*). For magnetic measurements the following compounds have been prepared: $Li_2MnF_5$ by solid-state reaction (v.s.), $Na_2MnF_5$ (*14*), $(NH_4)_2MnF_5$ (*15*), $SrMnF_5 \cdot H_2O$ (*16*), $BaMnF_5 \cdot H_2O$ (*16*), $Rb_2MnF_5 \cdot H_2O$ (*17*), and $Cs_2MnF_5 \cdot H_2O$ (*13*) from aqueous hydrofluoric acid solutions as given in the references. All powder samples were checked for purity by X-ray powder diagrams and chemical analyses of the F and Mn contents.

The most important structural parameters are summarized in Table III. A discussion of the influence of the Jahn–Teller effect and the structural relations are given elsewhere (*14*, *16*). The good conformity of bond lengths in this group of linear-chain compounds of ferrodistortive order allows a correlation to be set up between magnetic properties and only a single structural parameter, i.e., the bridge angle $\beta$. It is worth establishing that in contrast $KMnF_4 \cdot H_2O$ has an antiferrodistortive chain ($\beta = 137.7°$) and a mean intrachain exchange energy of $-5.9(5)$ K (*30*).

## Magnetism

With the aid of a vibrating sample magnetometer (Foner), the magnetic susceptibility of these polycrystalline pentafluoromanganates(III) has been measured from 4.2 to 300 K in an external magnetic field up to 20 kG. The observed broad maxima undoubtedly are due to short-range antiferromagnetic interaction within the –Mn–F–Mn linear chain. Choosing an isotropic Heisenberg Hamiltonian, we fitted a linear-chain model to the experimental data points. Although an exact result is not available for $S = 2$ systems, Fisher (*3*) has calculated the exact solution for a classical ($S = \infty$) linear chain, normalized for finite spins (*18*), which is given by

$$\chi(T) = \frac{Ng^2\beta^2S(S+1)}{3kT}\frac{(1+u)}{(1-u)}, \quad (1)$$

where

$$u = \coth K - K^{-1} \quad \text{and}$$

$$K = \frac{2JS(S+1)}{kT}.$$

The quantity $Ng^2\beta^2S(S+1)/3kT$ is the Curie law susceptibility for spin $S$.

In Eq. (1) it is assumed that the antiferromagnetic chains of $Mn^{3+}$ ions in the compound are essentially infinitely long. For finite Heisenberg chains, Fisher (*3*) shows that Eq. (1) is replaced by the more general result

$$\chi = \frac{Ng^2\beta^2S(S+1)}{(n+1)3kT}\left((n+1)\frac{1+u}{1-u} - 2u\frac{1-u^{n+1}}{(-u)^2}\right), \quad (2)$$

where $N$ is the total number of spins and $n + 1$ the number of spins per chain. If $J < 0$ and $n + 1$ finite, Eq. (2) yields a behavior quite similar to that given by Eq. (1) except that as $T$ falls to sufficiently low values $\chi^{-1}$ will again begin to fall.

By choosing $n$, the exchange constant

TABLE IV

MAGNETIC PROPERTIES OF THE STUDIED ANTIFERROMAGNETIC HEISENBERG CHAINS[a]

| Compound | $\beta$ (°) | Exchange energy $J/k$ (K) | | | $n$ per chain | $g$ factor | $\mu_{eff}$ ($\mu_B$) (300 K) | $\theta$ (K) | $T(\chi_{max})$ (K) |
|---|---|---|---|---|---|---|---|---|---|
| | | HTE | FM | Mean | | | | | |
| $Li_2MnF_5$ | 121.5 | −6.0 | −6.3 | −6.15 | ∞ | 2.02 | 4.58 | −66 | 30.5 |
| $Na_2MnF_5$ | 132.5 | −8.1 | −8.4 | −8.25 | 50 | 1.84 | 4.01 | −91 | 43 |
| $SrMnF_5$ | 139.8 | −9.9 | −10.3 | −10.1 | 45 | 1.88 | 3.99 | −134 | 53 |
| $(NH_4)_2MnF_5$ | 143.4 | −10.0 | −11.2 | −10.6 | 160 | 1.93 | 4.00 | −153 | 60 |
| $BaMnF_5 \cdot H_2O$ | 147.7 | −12.2 | −13.5 | −12.8 | 200 | 1.95 | 3.99 | −181 | 69 |
| $Rb_2MnF_5 \cdot H_2O$ | 175.8 | −18.8 | −20.0 | −19.4 | ∞ | 2.02 | 4.00 | −428 | 117 |
| $Cs_2MnF_5 \cdot H_2O$ | 180.0 | −16.5 | −19.0 | −17.8 | ∞ | 2.01 | 4.00 | −331 | 115 |

[a] Listed are the bridge angle $\beta$, the intrachain exchange energies $J/k$ derived from the high-temperature expansion (HTE) and the Fisher model (FM), the chain length $n$, the $g$ factor calculated from HTE-fitting procedure, the effective magnetic moment $\mu_{eff}$ calculated from the experimental data, the Curie–Weiss temperature $\theta$, and the temperature $T(\chi_{max})$ at which the maxima in the magnetic susceptibility occur.

$J/k_B$, and the Landé $g$ factor properly, our experimental data can be fitted to the classical approximations of Eqs. (1) and (2). The best-fit values thus obtained are shown in Table IV. In Figs. 3 and 4 we have plotted as a solid line the reciprocal magnetic susceptibility for these calculated parameters, together with the experimental results. It is easy to conceive that imperfections exist in a real crystal which may limit the average effective chain length to the assumed and calculated magnitude $n$.

An alternative approach is the high-temperature series expansion method

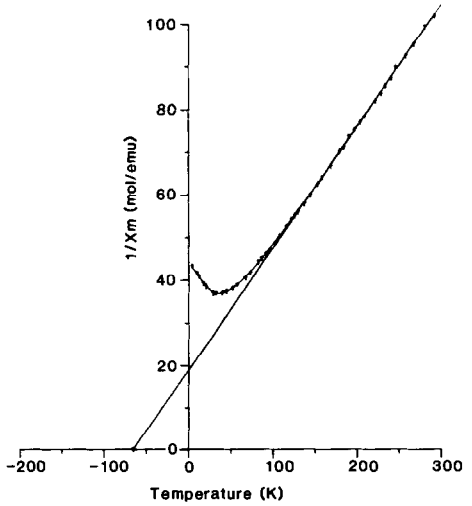


FIG. 3. Temperature dependence of the inverse magnetic susceptibility per mole for a powder of $Li_2MnF_5$. The straight line represents the Curie–Weiss law from data with $T > 150$ K and the solid curve has been calculated on the basis of the Fisher model (see Eqs. (1) and (2) and Table IV).

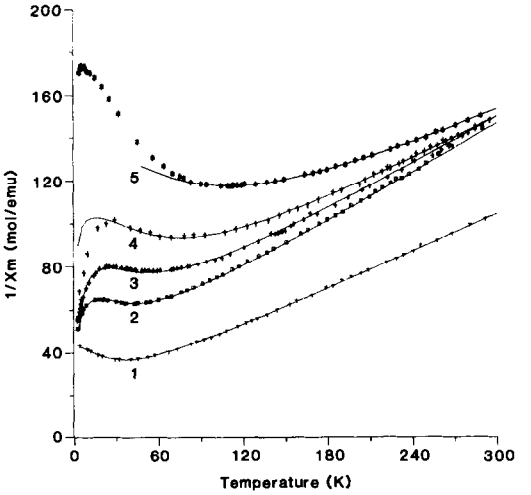


FIG. 4. Temperature dependence of the inverse magnetic susceptibility per mole in (1) $Li_2MnF_5$, (2) $Na_2MnF_5$, (3) $SrMnF_5 \cdot H_2O$, (4) $BaMnF_5 \cdot H_2O$, and (5) $Cs_2MnF_5 \cdot H_2O$. The solid curves have been calculated as in Fig. 3. The resulting parameters are listed in Table IV.

(HTE) for the susceptibility. In this approximation, the reciprocal of the reduced susceptibility is expanded in ascending powers of the reciprocal of the reduced temperature $T_r = kT/|J|$,

$$\chi_r = \frac{Ng^2\beta^2 3T_r}{J\chi S(S+1)} \sum_{m=0}^{m=\infty} (-1)^m \frac{b_m}{T_r^m}. \quad (3)$$

For an $S = 2$ Heisenberg linear chain there are six terms ($m = 0$–$6$) ($b1 = -8.0$; $b2 = 36.0$; $b3 = -72.5$; $b4 = -117.0$; $b5 = 942.0$; $b6 = 236.0$) available in the expansion, and this has been calculated by Rushbrooke and Wood assuming that interactions occur only between nearest neighbors (*19*). The calculated values of $|J|/k_B$ and $g$ from the best fit or Eq. (3) to the experimental data practically coincide in the temperature range $T_r \geq 6$ with the classical approach (see Table IV).[2] However, it is first worth noting that Eq. (3) was fitted to the experimental data and then the derived parameters $J/k$ and $g$ were used as starting parameters for calculating the magnetic susceptibility on the basis of the Fisher model.

The results as analyzed by use of both high- and low-temperature theoretical methods are listed in Table IV. In this table the compounds are listed according to increasing bridge angle $\beta$, and also shown are the mean chain length $n$, the effective magnetic moment at 300 K, the Curie–Weiss temperature $\theta$, and the temperature $T(\chi_{max})$ at which the maximum of the magnetic susceptibility occurs (*20*).

It is worth establishing that in contrast to the series expansion method (*19*), the prediction of the Fisher model (*3*) completely covers the temperature range in which the broad minimum of the inverse susceptibility occurs. One can see that at high temperatures there is no appreciable difference with the ideal behavior of a linear chain, but as the temperature is lowered some deviations from the isolated chain predicted by the Heisenberg model are observed. The fact that the agreement with decreasing bridge angle $\beta$ is better seems to suggest the presence of interchain coupling or long-range order effects. Kida and Watanabe (*24*) revealed by a single-crystal study that even for $(NH_4)_2MnF_5$, a 3-dimensional magnetic order exists below 7.5 K. Lacking any appropriate single crystals, we studied as a representative example the effect of dimensionality on the magnetic properties with the aid of $^{57}Fe$ Mössbauer spectroscopy in a powder probe of $Rb_2Mn_{0.99}Fe_{0.01}F_5 \cdot H_2O$ (*21*). In zero and external magnetic fields up to 5 T there is clear evidence of a 3-dimensional magnetic order at 4.2 K. With increasing temperature the magnetic hyperfine field of 511 kOe at 4.2 K is continuously reduced and vanishes near 26 K. In an extended temperature range below and above 26 K, one observes relaxation effects on the Mössbauer patterns obviously due to nonlinear excitations (solitons) in a quasi-1-dimensional antiferromagnet (*25*). A detailed Mössbauer study of $^{57}Fe$ in $Rb_2Mn_{1-x}Fe_xF_5 \cdot H_2O$ is now under consideration.

On the other hand, the differences between the experimental data and theory (see Fig. 4) may be caused by the influence of anisotropy effects at low temperatures masking the 3-dimensional phase transition as seen above. The zero-field splitting is apparently small in manganese(III) chain compounds (*26*). These effects were not considered by the isotropic Heisenberg model.

### Intrachain Exchange Interaction

Contrary to a simple expectation, the absolute value of the intrachain exchange energy $J$ increases with increasing Mn–Mn distances. This indicates that the super-

[2] Similar values of $J/k$ for selected linear-chain fluoromanganates(III) have been claimed by Emori *et al.* (*22*) and Nunez *et al.* (*23*).

exchange interaction depends to a great extent on the Mn–F–Mn bridge angle rather than the Mn–Mn or Mn–F distances (see Tables III and IV).

In accordance with the rules of Anderson (*27*), Goodenough (*28*), and Kanamori (*29*), the sign of superexchange interaction can be determined from the symmetry relation of atomic orbitals involved.

The electronic configuration of a $Mn^{III}$ ion in its high-spin state is $d_\varepsilon^3 d_{z^2}^1$. The Jahn–Teller distortion along the chain axis indicates that the half-occupied $d_z^2$ orbitals are all pointing in this direction. If Mn–F–Mn is linear, partial $\sigma$ bonds are formed by the $p_z$ orbital of fluorine and the $d_z^2$ orbital of manganese. Since these orbitals are nonorthogonal or bond forming, antiferromagnetic coupling results between these manganese ions. With decreasing angle Mn–F–Mn, the antiferromagnetic interactions obviously decrease as $\cos^2(\beta)$ owing to the decrease in the overlap of the $d_z^2$ and $p_z$ orbitals involved. The proper linearity of the function in Fig. 5 strongly supports the assumption of dominance of this $\sigma$-superexchange mechanism.

In addition to this, a superexchange interaction between the $d_{xz}$ and $d_{yz}$ orbitals of manganese forming $\pi$ bonds with the $p_x$ and $p_y$ orbitals of fluorine has to be taken into consideration. The resulting contribution to the superexchange interaction should be antiferromagnetic for the same reasons as above, but it is presumed to be weaker and less dependent on the Mn–F–Mn bridge angle. This effect may be indicated by the slight systematical deviations of the experimental data from the straight line (Fig. 5). On the other hand, it is worthwhile to establish that, at least in the range of very low bridge angles, a possible ferromagnetic superexchange contribution favored for 90° cation–anion–cation interaction predicted by Anderson (*27*) may reduce the antiferromagnetic coupling between the manganese ions in the same way as a consequence of decreasing bridge angle $\beta$. This argument may explain the larger moment in $Li_2MnF_5$ in comparison with the others in Table IV.

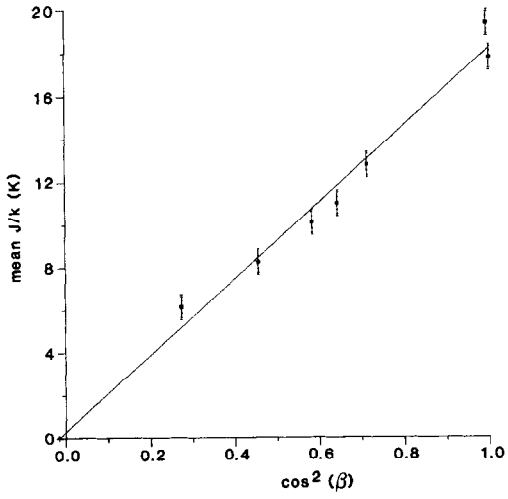


FIG. 5. Mean absolute value of the effective intrachain exchange energy $J/k$ (see Table IV) as a function of $\cos^2(\beta)$. The exchange energy $|J|/k$ for the $\sigma$-superexchange interaction approximately vanishes at $\beta = 90°$.

## Acknowledgments

The authors are grateful for the financial support from the Deutschen Forschungsgemeinschaft and the Fonds der Chemischen Industrie.

## References

1. C. DOMB, *Philos. Mag. Suppl.* **9,** 149 (1960).
2. J. C. BONNER AND M. E. FISHER, *Phys. Rev. A* **135,** 640 (1964).
3. M. E. FISHER, *Amer. J. Phys.* **32,** 343 (1964).
4. L. J. DE JONGH AND A. R. MIEDEMA, *Adv. Phys.* **23,** 1 (1974).
5. A. TRESSAUD AND J. M. DANCE, "Structure and Bonding," Vol. 52, Springer-Verlag, Berlin (1982); "Magneto-Structural Correlations in Exchange Coupled Systems" (R. D. Willett, D. Gatteschi, and O. Kahn, Eds.), Nato ASI Series, Reidel, Dordrecht (1985).
6. D. BABEL, *Comment. Inorg. Chem.* **5** (1986).

7. D. T. CROMER AND J. D. MANN, *Acta Crystallogr., Sect. A* **24,** 321 (1968).
8. D. T. CROMER AND D. LIBERMAN, *J. Chem. Phys.* **53,** 1891 (1970).
9. R. E. SCHMIDT, M. BIRKHAHN, AND W. MASSA, STRUX, Programmsystem zur Verarbeitung von Röntgendaten, Marburg (1980).
10. G. M. SHELDRICK, "SHELX76, Program for Crystal Structure Determination," Cambridge University, Cambridge, England (1976).
11. C. K. JOHNSON, "ORTEP, a Fortran Thermal-Ellipsoid Plot Program for Crystal Structure Illustrations," Report ORNL-3794, Oak Ridge, TN (1965).
12. W. MASSA AND F. HAHN, Tenth European Crystallographic Meeting, Wroclaw, Poland, August 7, 1986.
13. V. KAUCIC AND P. BUKOVEC, *Acta Crystallogr., Sect. B* **34,** 3337 (1978).
14. W. MASSA, *Acta Crystallogr., Sect. C* **42,** 644 (1986).
15. D. R. SEARS AND J. L. HOARD, *J. Chem. Phys.* **50,** 1066 (1969).
16. W. MASSA AND V. BURK, *Z. Anorg. Allg. Chem.* **516,** 119 (1984).
17. P. BUKOVEC AND V. KAUCIC, *Acta Crystallogr., Sect. B* **34,** 3339 (1978).
18. T. SMITH AND S. A. FRIEDBERG, *Phys. Rev.* **176,** 660 (1968).
19. G. S. RUSHBROOKE AND P. J. WOOD, *Mol. Phys.* **1,** 257 (1958); **6,** 409 (1963).
20. L. J. DE JONGH AND A. R. MIEDEMA, "Experiments on Simple Magnetic Model Systems," Taylor & Francis, London (1974).
21. J. PEBLER, unpublished measurements, 1986.
22. S. EMORI, M. INOUE, M. KISHITA, AND M. KUBO, *Inorg. Chem.* **8,** 1385 (1969).
23. P. NUNEZ, J. DARRIET, P. BUKOVEC, A. TRESSAUD, AND P. HAGENMULLER, *Mater. Res. Bull.* **22,** 661 (1987).
24. J. KIDA AND T. WATANABE, *J. Phys. Soc. Japan,* **34,** 952 (1973).
25. L. J. DE JONGH, *J. Appl. Phys.* **53,** 8018 (1982); R. C. THIEL, H. DE GRAF, AND L. J. DE JONGH, *Phys. Rev. Lett.* **47,** 1415 (1981).
26. W. E. HATFIELD, W. E. ESTES, W. E. MARSH, M. W. PICKENS, L. W. TER HAAR, AND R. R. WELLER, *in* "Extended Linear Chain Compounds" (J. S. Miller, Ed.), Vol. 3, Plenum, New York (1983).
27. P. W. ANDERSON, *Phys. Rev.* **79,** 350 (1950).
28. J. B. GOODENOUGH, "Magnetism and Chemical Bond," New York (1963).
29. J. KANAMORI, *J. Phys. Chem. Solids* **10,** 87 (1959).
30. W. MASSA AND J. PEBLER, 3rd European Conference on Solid State Chemistry, Regensburg, Germany, 1986, Abstracts Vol. 7, p. 175.